Supplementary Material (ESI) for Journal of Analytical Atomic Spectrometry
This journal is © The Royal Society of Chemistry 2012

SUPPORTING INFORMATION

ANALYSIS OF BIODIESEL AND OIL SAMPLES BY ON-LINE CALIBRATION USING A FLOW BLURRING® MULTINEBULIZER ON ICP OES WITHOUT OXYGEN ADDITION

*Miguel Ángel Aguirre, Nikolay Kovachev, Montserrat Hidalgo and Antonio Canals**

*Departamento de Química Analítica, Nutrición y Bromatología e Instituto Universitario de Materiales, Universidad de Alicante, Apdo. 99, Alicante E-03080, Spain. *E-mail: a.canals@ua.es*

Aerosol characterization

Fig. S1 on ESI† shows the accumulated percent volume of primary and tertiary aerosols produced by the SSI and the FBMN-based systems under optimized conditions of gas and liquid flow rates. For the FBMN-based system, primary aerosols generated by each nozzle of the nebulizer from either organic or aqueous solutions were studied separately (i.e., organic aerosol generated by nozzle 1 and aqueous aerosols generated by nozzles 2 and 3). Tertiary aerosol produced by the FBMN-based system, consisting on a mixture of organic and aqueous aerosols generated from the different nozzles, was measured at the exit of a 2.0 mm i.d. injector tube connected to the cyclonic-type spray chamber, pursuant to the conditions used in ICP OES measurement. With the MM nebulizer and the corresponding SSI system, only primary and tertiary organic aerosols were studied. In this case, tertiary organic aerosol was measured at the exit of the 0.8 mm i.d. injector tube connected to the same cyclonic spray chamber.

Fig. S1 on ESI† shows how primary aqueous aerosols generated with the FBMN from nozzles 2 and 3 have very similar characteristics, evidencing a good matching between these two nozzles. As expected, aerosol droplets generated from organic solutions (FBMN nozzle 1) are slightly smaller than those generated from aqueous solutions. In this case, the mean reasons for this behaviour are the lower viscosity and surface tension of organic solvent and the lower liquid uptake rate through nozzle 1 of the FBMN[1-6]. According to Fig. S1 on ESI†, practically all the organic aerosol volume is contained in droplets smaller than 33 µm, whereas all the aqueous aerosol volume is contained in droplets smaller than 42 µm. The aforementioned figure also shows how that MM nebulizer generates coarser droplets than FBMN, with practically all the organic aerosol volume contained in droplets smaller than 114 µm.

The analysis of accumulated percent volume of tertiary aerosol obtained for the two systems reveals that droplets larger than approximately 20 µm are, in both cases, removed by the spray chamber. This result can be associated with the spray chamber cut-off diameter (d_c) if neglecting the injector tube contribution to the obtained tertiary aerosol distribution. The percent volume of primary aerosols contained in droplets smaller than the d_c (20 µm) was 96%, 88% and 85% for nozzles 1, 2 and 3 of the FBMN, respectively, and 27% µm for the MM nebulizer, which predicts a higher spray chamber filtering action for the SSI system.

It is also interesting to evaluate the percent volume of aerosol droplets that, entering the ICP torch, contributes positively to signal. According to the literature, droplets larger than approximately 8 µm in diameter moving at relatively high velocities, normally contribute negatively to the signal-to-background ratio in ICP spectrometry[7]. From Fig. S1 on ESI† it can be seen than the percentage of the aerosol volume contained in droplets smaller than 8 µm was approximately equal for the two systems (58% and 64% for FBMN-based system and the SSI system, respectively). However, the mean velocities of the tertiary aerosol produced by the FBMN-based system was lower (4 m s^{-1}) than that of the SSI system (11 m s^{-1}). This fact could be due to the i.d. of the injector tube (see Table S1 on ESI†) and could positively contribute to the signal obtained with the multinebulization system.

Other useful information regarding the obtained aerosols (i.e., Sauter mean diameter ($D_{3,2}$), axial mean velocity (V_m), volume median diameter (D_{50}) and droplet diameter containing 99% of the total aerosol volume (D_{99})) is also available in Table S3 on ESI†.

Lastly, it is noteworthy that the results obtained correspond to measurements carried out with both nebulizers working at the optimized gas and liquid flow rates for ICP OES measurements of organic samples (see Table S1 on ESI†), and not under the working conditions recommended by the MM manufacturer. To reach optimum conditions in ICP OES, the MM nebulizer needs a higher carrier gas supply than FBMN for the same 100 µl min^{-1} liquid sample inlet (i.e., 800 mbar (0.4 L min^{-1}) and 400 mbar (0.2 L min^{-1} per each nozzle, approximately) for the MM nebulizer and FBMN, respectively). This fact makes the use of Flow Blurring® nebulization devices ideal for a multiple nozzle platform in ICP OES analysis, because the efficient mixing between the gas and liquid phases leads to energy-efficiency improvements over other pneumatic nebulizers.

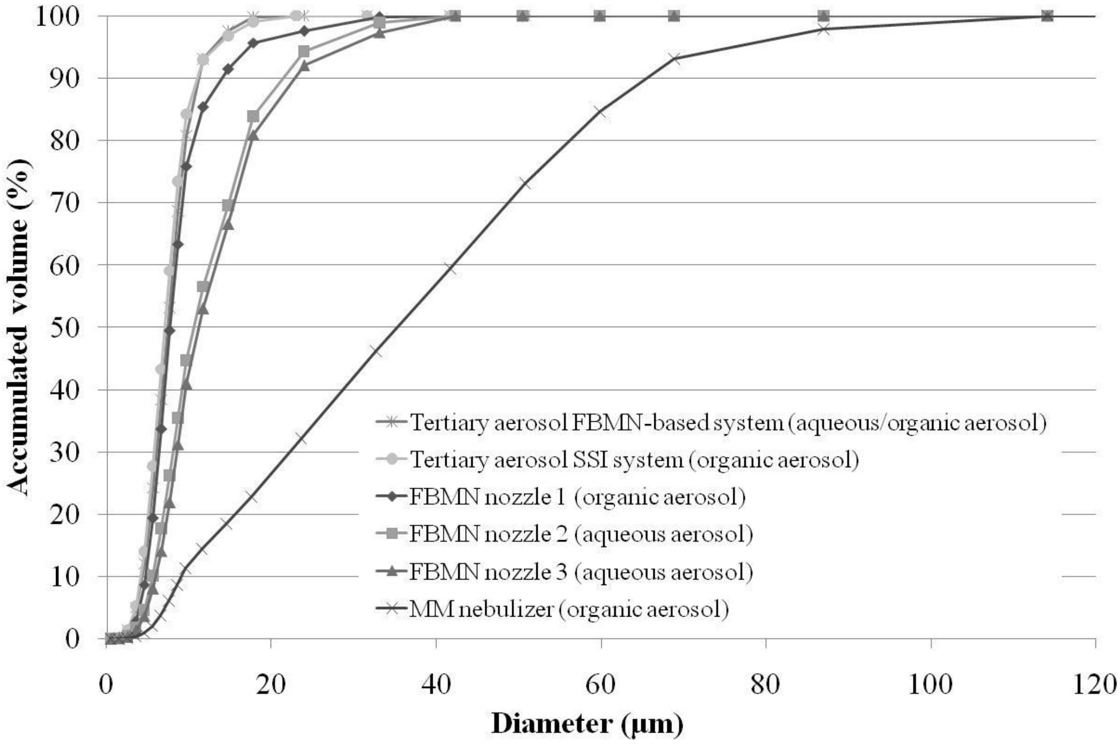

Fig. S1. Accumulated percent volume of primary and tertiary aerosols produced by the FBMN-based system and the SSI system under optimized gas and liquid flow rate conditions (Table S1 on ESI†).

Electronic Supplementary Material (ESI) for Journal of Analytical Atomic Spectrometry

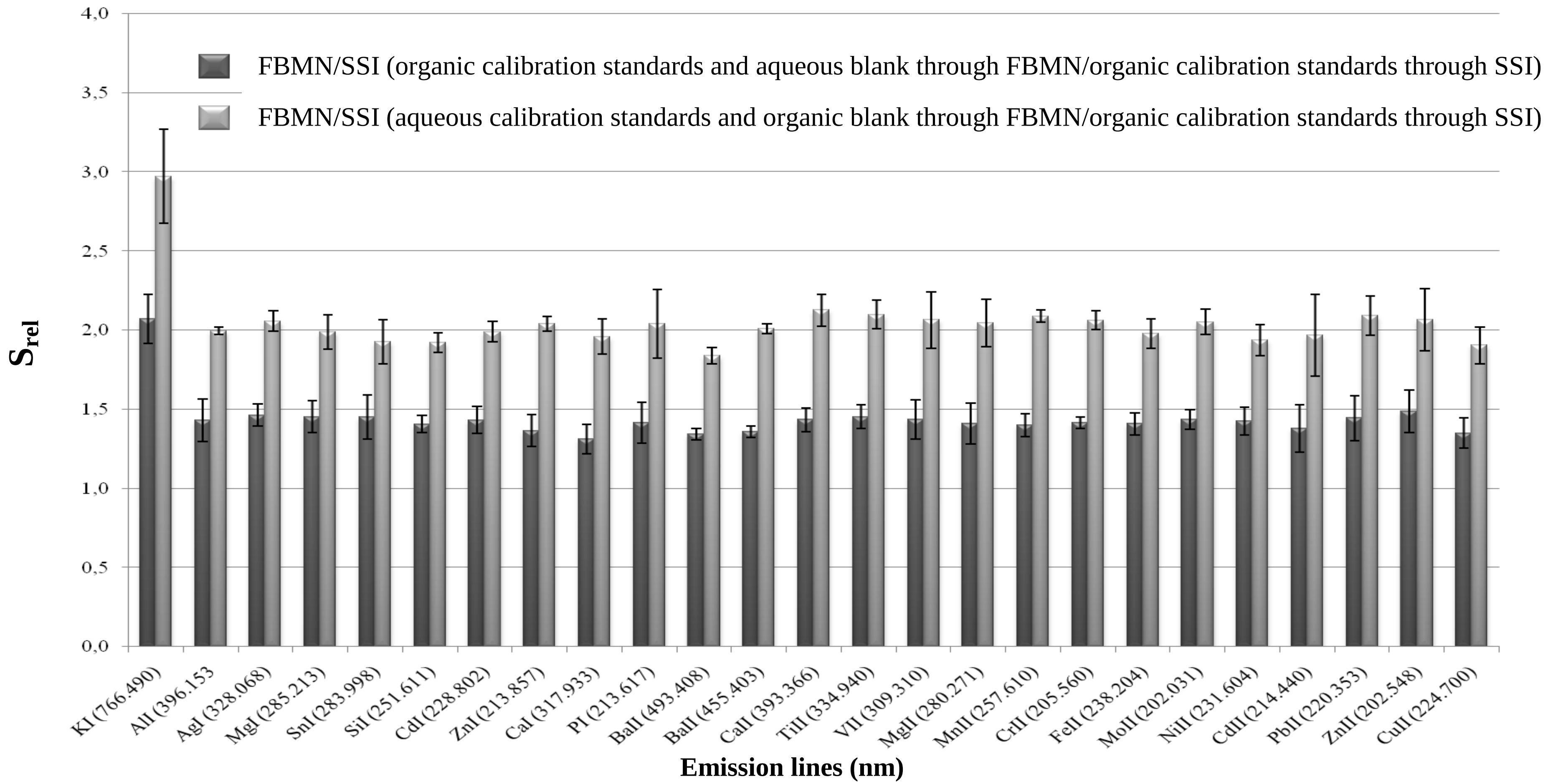

Fig. S2. Relative sensitivity of FBMN and SSI systems ($S_{rel}=S_{FBMN\text{-based system}} / S_{SSI\ system}$) in two different sensitivity evaluation experiments (see main text for explanation).

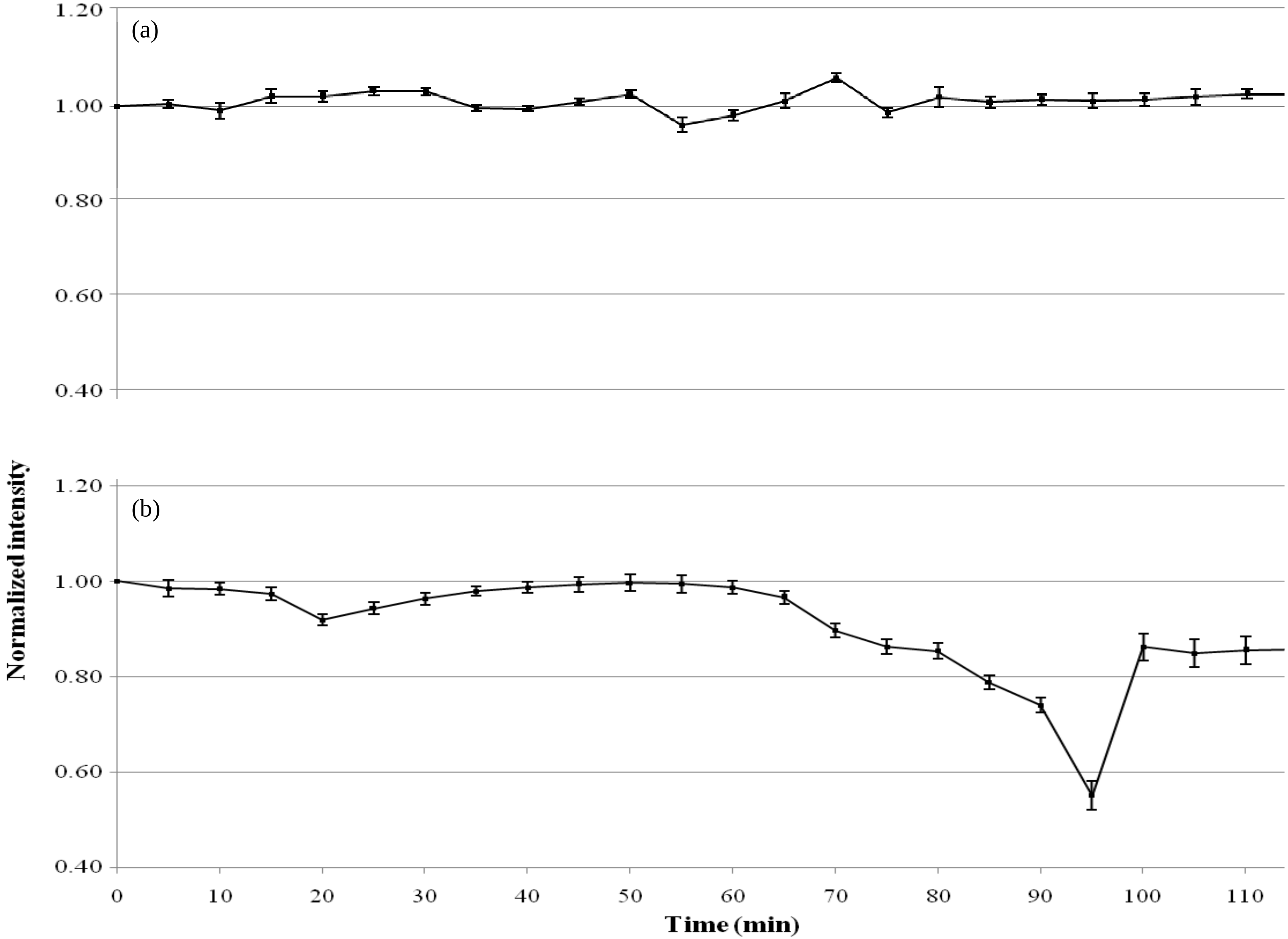

Fig. S3. Evolution of the emission signal of the average of all emission lines evaluated during two hours of continuous nebulization with (a) FBMN-based system (1 µg g^{-1} of organic standard solution at 100 µL min^{-1} and 1 µg g^{-1} of aqueous blank at 400 µL min^{-1}) and (b) SSI system (1 µg g^{-1} of organic standard solution at 100 µL min^{-1}).

Table S1. ICP OES operating conditions.

Plasma parameters	**FBMN-based system**	**SSI system**
Outer gas flow (L min^{-1})	15	15
Intermediate gas flow (L min^{-1})	0.2	1.2
RF power (W)	1350	1350
Integration time (s)	Variable	Variable
Read time (s)	Variable	Variable
Number of replicates	5	5
Viewing mode	Axial	Axial
Sample introduction system		
Nebulizer type	FBMN	MicroMist
Spray chamber	cyclonic	cyclonic
Gas flow rate (L min^{-1})	0.60	0.40
Pressure gas supplied (mbar)	400	800
Total liquid uptake rate (µL min^{-1})	500	100
Organic sample uptake rate (µL min^{-1})	100	100
Aqueous standard uptake rate (µL min^{-1})	400	-
Injector tube (mm. id)	2.0	0.8

Table S2. Emission lines and energy values.

Emission line (nm)	Excitation Energy (eV)	Ionization Energy (eV)	E_{sum} (eV)
KI (766.490)	1.62	-	1.62
NaI (589.592)[a]	2.10	-	2.10
NaI (588.995)[b]	2.11	-	2.11
AlI (396.153)	3.14	-	3.14
AgI (328.068)	3.78	-	3.78
MgI (285.213)	4.34	-	4.34
SnI (283.998)	4.78	-	4.78
SiI (251.611)	4.95	-	4.95
CdI (228.802)	5.41	-	5.41
ZnI (213.857)	5.80	-	5.80
CaI (317.933)	7.04	-	7.04
PI (213.617)	7.22	-	7.22
BaII (493.408)	2.51	5.21	7.72
BaII (455.403)	2.72	5.21	7.93
CaII (393.366)	3.15	6.11	9.26
TiII (334.940)	3.74	6.82	10.56
VII (309.310)	4.40	6.74	11.14
MgII (280.271)	4.42	7.65	12.07
MnII (257.610)	4.81	7.44	12.25
CrII (205.560)	6.03	6.77	12.80
FeII (238.204)	5.20	7.87	13.07
MoII (202.031)	6.13	7.10	13.23
NiII (231.604)	6.39	7.64	14.03
CdII (214.440)	5.78	8.99	14.77
PbII (220.353)	7.37	7.42	14.79
ZnII (202.548)	6.12	9.39	15.51
CuII (224.700)	8.23	7.73	15.96

[a]only measured with FBMN-based system
[b]only measured with SSI system

Table S3. Primary and tertiary aerosol characterization of MM nebulizer, FBMN, SSI system and FBMN-based system.

Primary aerosol	$D_{3,2}$[a]	V_m[b]	D_{50}[c]	D_{99}[d]
FBMN nozzle 1 (organic aerosol)	10.7±0.3	12.1±0.2	7.7±0.3	30±5
FBMN nozzle 2 (aqueous aerosol)	16.5±0.3	18.1±0.3	10.6±0.8	34±4
FBMN nozzle 3 (aqueous aerosol)	16.67±0.12	18.0±0.4	11.2±0.2	39±2
MM nebulizer (organic aerosol)	40±2	35.4±0.2	36±3	102±21
Tertiary aerosol	$D_{3,2}$[a]	V_m[b]	D_{50}[c]	D_{99}[d]
FBMN-based system	7.80±0.14	3.7±0.2	7.4±0.2	16.8±1.0
SSI system	8.06±0.09	11.14±0.08	7.07±0.10	17.9±0.7

[a]Sauter mean diameter (μm).
[b]Axial mean velocity (m s^{-1}).
[c]Volume median diameter (μm).
[d]Droplet diameter containing 99 % of the total aerosol volume (μm).

Table S4. RSD (%) values for short-term precision (STP) at three different concentration levels and for long-term precision (LTP) using the SSI and FBMN systems.

	RSD (%)							
	SSI system				FBMN-based system			
	STP (%)[a]			LTP (%)[b]	STP (%)[a]			LTP (%)[b]
Emission lines (nm)	0.4[c]	1.2[c]	2.0[c]		0.4[c]	1.2[c]	2.0[c]	
KI (766.490)	3	3	3	12	2	1.2	1.3	2
NaI (589.592)	-	-	-	-	1.4	2	2	2
NaI (588.995)	2	2	3	11	-	-	-	-
AlI (396.153)	3	3	2	12	1.4	1.2	1.5	2
AgI (328.068)	1.5	3	2	10	2	1.3	1.5	2
MgI (285.213)	3	3	2	12	2	1.5	1.2	2
SnI (283.998)	2	2	2	12	2	1.5	2	2
SiI (251.611)	2	2	2	12	2	1.4	2	2
CdI (228.802)	1.3	2	2	11	1.4	2	2	2
ZnI (213.857)	2	2	2	11	2	1.4	2	2
CaI (317.933)	4	2	2	12	1.4	1.5	1.4	2
PI (213.617)	2	2	2	13	2	2	2	2
BaII (493.408)	2	2	2	12	0.7	0.9	0.8	2
BaII (455.403)	2	2	2	12	1.1	1.2	1	1.5
CaII (393.366)	2	1.2	2	11	1.5	0.9	2	2
TiII (334.940)	2	2	2	11	2	2	2	2
VII (309.310)	5	4	2	12	1.4	1	1.5	2
MgII (280.271)	2	2	2	11	0.9	1.3	1.1	2
MnII (257.610)	2	3	2	12	1.5	1.4	1.3	2
CrII (205.560)	2	2	3	12	2	1.3	2	2
FeII (238.204)	2	2	3	11	1.3	2	1.2	2
MoII (202.031)	2	1.5	2	12	2	2	2	2
NiII (231.604)	3	2	3	12	2	2	2	2
CdII (214.440)	3	2	3	11	0.6	1.4	1	2
PbII (220.353)	4	4	4	12	2	2	1.4	2
ZnII (202.548)	5	4	3	12	1.5	1.4	2	2
CuII (224.700)	2	2	2	12	1.4	2	2	2

[a]The RSD values of the signal over one minute (n=5 replicates).
[b]The RSD values of the signal over two hours (n= 600 replicates).
[c]In μg g^{-1}.

.

Table S5. Limits of detection (LOD) obtained using conventional standard addition calibration with the SSI system and on-line standard addition calibration with the FBMN-based system.

Emission lines (nm)	LOD (ng g^{-1})	
	SSI system	FBMN-based system
KI (766.490)	6	1.3
NaI (589.592)	-	1.4
NaI (588.995)	9	-
AlI (396.153)	12	6
AgI (328.068)	1.5	0.2
MgI (285.213)	0.8	0.14
SnI (283.998)	9	1.4
SiI (251.611)	4	2
CdI (228.802)	1.3	0.3
ZnI (213.857)	1.2	0.4
CaI (317.933)	6	1.0
PI (213.617)	8	4
BaII (493.408)	0.4	0.11
BaII (455.403)	1.0	0.12
CaII (393.366)	6	2
TiII (334.940)	2	0.12
VII (309.310)	2	0.7
MgII (280.271)	1.2	0.3
MnII (257.610)	0.3	0.04
CrII (205.560)	5	2
FeII (238.204)	2	0.6
MoII (202.031)	10	4
NiII (231.604)	8	1.0
CdII (214.440)	2	0.4
PbII (220.353)	14	7
ZnII (202.548)	2	0.8
CuII (224.700)	5	1.2

Table S6. Concentration (ng g^{-1}) and recovery values (%) of the three real samples of diesel using the SSI system.

Emission lines (nm)	LOQ (ng g^{-1}) Diluted oil sample	LOQ (ng g^{-1}) 100% Biodiesel	Petrol station 1 Found value[a,b]	Petrol station 1 SR (%)[c]	Petrol station 2 Found Value[a,b]	Petrol station 2 SR (%)[c]	Petrol station 3 Found value[a,b]	Petrol station 3 SR (%)[c]
AgI (328.068)	5	20	<LOQ	92-104	<LOQ	85-103	25.1±0.6	100-114
AlI (396.153)	41	64	<LOQ	97-112	440±15	84-102	540±22	93-109
BaII (455.403)	3	4	<LOQ	89-112	<LOQ	98-113	4.08±0.04	87-109
BaII (493.408)	1	3	<LOQ	97-108	<LOQ	93-109	4.00±0.04	94-106
CaI (317.933)	20	30	61.5±1.3	93-107	48.4±0.9	93-103	30.8±0.4	98-112
CaII (393.366)	19	31	62.1±1.1	95-109	47.0±0.4	94-105	31.6±0.2	91-101
CdI (228.802)	4	11	<LOQ	89-104	44.6±0.5	91-101	68.2±0.9	92-104
CdII (214.440)	7	8	<LOQ	97-113	45.3±1.0	87-101	69.6±1.4	99-114
CrII (205.560)	15	25	<LOQ	93-110	<LOQ	98-109	<LOQ	91-108
CuII (224.700)	16	33	455±24	93-112	354±16	91-101	379±7	84-106
FeII (238.204)	5	9	<LOQ	91-114	19.3±0.2	88-102	<LOQ	95-104
KI (766.490)	21	24	<LOQ	90-101	25.4±0.8	95-114	<LOQ	98-108
MgI (285.213)	3	4	<LOQ	88-106	5.73±0.12	91-104	18.6±0.4	89-103
MgII (280.271)	4	5	<LOQ	93-106	5.86±0.06	93-108	18.3±0.3	98-110
MnII (257.610)	1	1.4	<LOQ	90-109	7.0±0.3	88-102	16.2±0.2	91-102
MoII (202.031)	34	94	<LOQ	89-103	<LOQ	90-101	<LOQ	92-104
NaI (588.995)	29	33	<LOQ	97-100	88±2	85-103	36.5±0.2	98-107
NiII (231.604)	27	45	<LOQ	91-106	<LOQ	97-109	<LOQ	99-109
PbII (220.353)	47	60	137±4	83-101	453±21	94-108	836±33	89-103
PI (213.617)	25	58	466±9	93-111	<LOQ	92-101	<LOQ	87-105
SiI (251.611)	13	37	<LOQ	93-106	252±7	89-106	163±4	95-105
SnI (283.998)	29	50	438±24	97-114	<LOQ	86-101	142±3	83-104
TiII (334.940)	7	9	<LOQ	96-105	<LOQ	94-109	<LOQ	93-101
VII (309.310)	7	12	<LOQ	100-112	<LOQ	91-108	<LOQ	95-108
ZnI (213.857)	4	7	<LOQ	98-108	<LOQ	88-104	<LOQ	99-110
ZnII (202.548)	6	7	<LOQ	89-100	<LOQ	91-101	<LOQ	89-100

[a]The uncertainty values are the estimated standard deviation of the extrapolated concentration[8]. [b]In ng g^{-1}.
[c]Spike recovery of 1 µg g^{-1}.

.

References

1. A. W. Boorn and R. F. Browner, in *Inductively Coupled Plasma Emission Spectroscopy, Pt. 2: Applications and Fundamentals*, Boumans, P. W. J. M. (ed), (John Wiley & Sons, 1987). Ch. 6, pp. 151-216.
2. A. W. Boorn and R. F. Browner, *Anal. Chem.*, 1982, **54**, 1402–1410.
3. J. Farino and R. F. Browner, *Anal. Chem.* , 1984, **56**, 2709–2714.
4. J. Farino, J. R. Miller, D. D. Smith and R. F. Browner, *Anal. Chem.* , 1987, **59**, 2303–2309.
5. A. Canals, V. Hernandis and R. F. Browner, *J. Anal. At. Spectrom.*, 1990, **5**, 66–61.
6. J. Mora, V. Hernandis and A. Canals, *J. Anal. At. Spectrom.*, 1991, **6**, 573–579.
7. A. Montaser, M. G. Minnich, H. Liu, A. G. T. Gustavsson and R. F. Browner, in *Inductively Coupled Plasma Mass Spectrometry*, A. Montaser, Ed. (Wiley-VCH, New York, 1998). Ch. 5, pp. 335-420.
8. J. N. Miller and J. C. Miller, in *Statistics and Chemometrics for Analytical Chemistry*, Prentice Hall, Harlow, UK, 2005. Ch. 2, pp. 107-149.